# POOL BOILING HEAT TRANSFER ENHANCEMENT USING MICRO-FIN SURFACES AND DIELECTRIC FLUIDS

**Igor Seicho Kiyomura[1], Jéssica Martha Nunes[1], Reinaldo Rodrigues de Souza[1] and Elaine Maria Cardoso[1,2]***

[1]UNESP – São Paulo State University, School of Engineering, Post-Graduation Program in Mechanical Engineering, Av. Brasil, 56, 15385-000, Ilha Solteira, SP, Brazil
[2]UNESP – São Paulo State University, Campus of São João da Boa Vista

## ABSTRACT

One promising way to enhance the heat transfer coefficient (HTC) and the critical heat flux (CHF) is modifying the heating surface morphology by using machining techniques, coating, and chemical processes. Micro-structured surfaces, *i.e.*, surfaces with the presence of micro-pillars on the surface, provide small perturbations in the liquid, affecting the vapor bubbles dynamic. These structures increase the heating surface area and change the fluid flow. Micro-fins can have different shapes and sizes and can be arranged in different patterns to improve heat transfer. This study aims to evaluate experimentally the thermal performance of different micro-fin surfaces by using HFE-7100 as working fluid. The square-micro pillar arrays were etched on a plain copper surface through the micro-milling process. Squares micro-fins of different length scales (i.e., height and side length) were uniformly spaced on the plain copper surface. The inter-fin space had the same value, 250 μm, for all surfaces in order to control the effective roughness, $R_{eff}$, defined as the ratio of the area in contact with the liquid to the projected area. Micro-fin surfaces intensify the HTC as compared to the plain surface and the number of fins is the main factor for the HTC enhancement; if the number of micro-fins is constant, the larger the effective roughness the higher the heat transfer performance. Additionally, the capillary-wicking ability increases and it also improves the HTC and the dryout heat flux due to the prevention of hotspots in the micro-fin surface. Thus, the surface thermal behavior is a function of the surface morphology and its surface capillary wicking.

**KEYWORDS:** micro-pillars, effective roughness, pool boiling, heat transfer coefficient, HFE-7100.

## 1. INTRODUCTION

Recent developments in microsystems have made it possible to increase the processing capacity of various electronic devices with a continuous reduction in their size. However, due to the technology advance and the growth of processing capacity, the heat dissipated per unit area in such devices increased significantly, Demir et al. [1].

Microstructured surfaces, *i.e*., surfaces with the presence of micro-pillars on the surface, provide small perturbations in the liquid, affecting the vapor bubbles dynamic. These structures increase the heating surface area and change the fluid flow. Micro-fins can have different shapes and sizes and can be arranged in different patterns to improve heat transfer, Liang et al. [2]. Cao et al. [3] studied different types of modified surfaces; the authors analyzed micro-finned silicon surfaces by the dry etching method. The tests were performed in the pool boiling at atmospheric pressure using FC-72 as the working fluid. The results showed that micro-finned surfaces could give a considerable increase in the boiling heat transfer in comparison to smooth surfaces.

*Corresponding Author: elaine.cardoso@unesp.br

The dynamics of growth and development of vapor bubbles on the heated surface are also influenced by the dimensions of the pillars. Dong et al. [4] compared the performance of silicon surfaces with microstructures and nanostructures. The results showed that the surfaces with microstructures had much higher density of active nucleation sites. However, nanostructures can accelerate the bubble departure by decreasing bubble diameter, preventing the formation of a vapor blanket at high heat fluxes. Sinha-Ray et al. [5] studied pool boiling of HFE-7300 and DI water on bare copper surface and copper surface covered with supersonically-blown or electrospun polymer nanofibers. It was shown that nanofibers generated large amounts of small pores, facilitating nucleation. Compared with DI water, HFE-7300 has a lower surface tension and saturation temperature and the onset of nucleate boiling appears at a smaller superheat.

In order to increase the useful area of the structured surfaces, geometric parameters such as height, width, and distance from one pillar to another are being studied by Cooke and Kandlikar [6]. The researchers reported that geometries with wider, deep channels and thin fins are responsible for better heat transfer performance.

In the results obtained by Cao et al. [3], the authors explain that a small channel is good for liquid supply due to a large capillary pressure, while a large channel is good for vapor escape due to a small hydraulic resistance. It is known that the micro-pin fins can promote liquid supply because of the microchannels generated by the pin fins, Kim et al. [7] and Kim et al. [8].

Therefore, the present work brings new perceptions of the microstructured surfaces in the boiling process and, consequently, in the HTC, making it possible to establish basic design guidelines for new surface technologies with high heat removal capacity for advanced applications in thermal management.

## 2. MICROSTRUCTURE SURFACE

Squares micro-fins of different length scales (*i.e.*, height and side length) were uniformly spaced on the plain copper surface, Fig. 1. The inter-fin space had the same value, 250 μm, for all surfaces in order to control the effective roughness, $R_{eff}$, defined as the ratio of the area in contact with the liquid to the projected area, as presented by Dong et al. [4] and Chu et al. [9].

The square-micro pillar arrays were etched on a plain copper surface through micro-milling process by using CNC precision machining, in the Manufacturing Process Laboratory/School of Engineering of São Carlos (LAMAFE/EESC-USP), by Prof. Dr. Alessandro Roger Rodrigues.
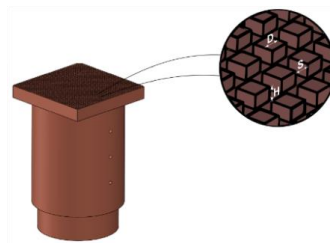


| Surface | Height, H (μm) | Side Length, D (μm) | Spacing, S (μm) | $R_{eff}$ | Fin number |
|---------|----------------|---------------------|-----------------|-----------|------------|
| Plain/Smooth Surface | - | - | - | 1 | - |
| Micro_Fin_n1 (M1) | 200 | 250 | 250 | 1.80 | 1024 |
| Micro_Fin_n2 (M2) | 150 | 250 | 250 | 1.60 | 1024 |
| Micro_Fin_n3 (M3) | 200 | 300 | 250 | 1.79 | 841 |
| Micro_Fin_n4 (M4) | 150 | 300 | 250 | 1.60 | 841 |

*Ratio of the top surface area of micro-fins to the projected area of the sample.
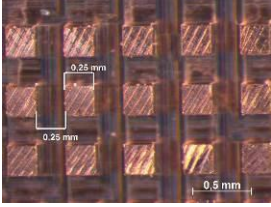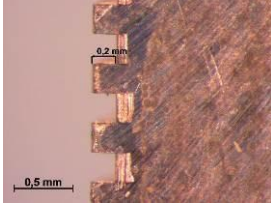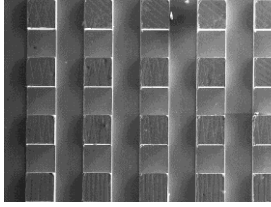
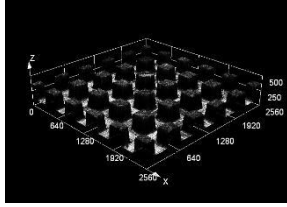$$R_{eff} = 1 + \left[ \frac{4DH}{(S+D)^2} \right]$$
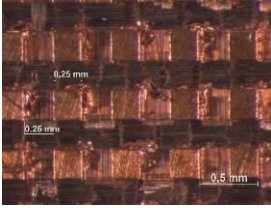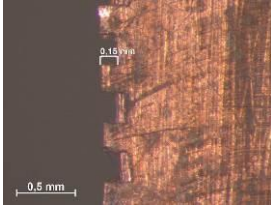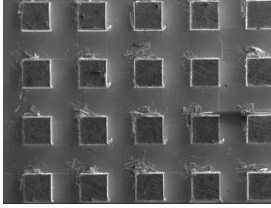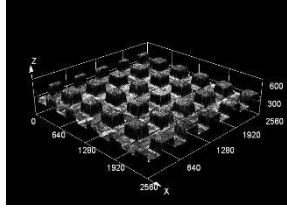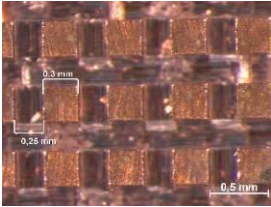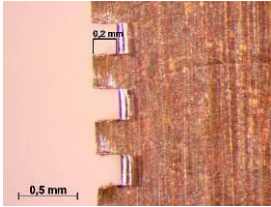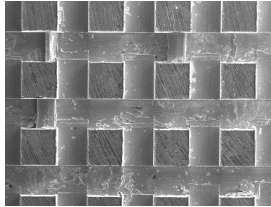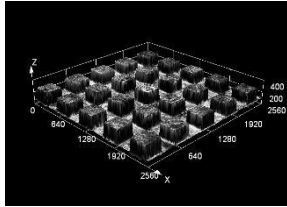
**Fig. 1** Schematic drawing of the microstructured surface.

For the geometric characterization of microstructures, three different microscopy techniques were used:

- Scanning Electron Microscopy (SEM), using an EVO LS15 Zeiss®;
- Optical Microscopy (STEREO), using a Zeiss® SteREO DiscoveryV8;
- Confocal microscopy, using an Olympus LEXT OLS 4000;

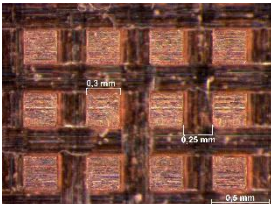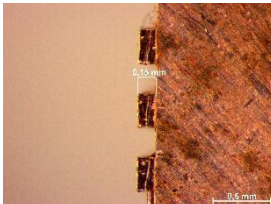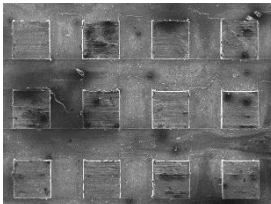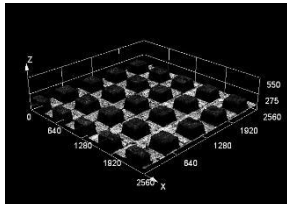These techniques were used to obtain the images presented in Table 1, which permits the verification of the finishing characteristics of the manufacturing process, and the established parameters of the square micro-fins, such as, height, width, and inter-fins space.

**Table 1** Structural characterization of the micro-fin array surfaces.

| STEREO | | SEM | Confocal Microscopy |
|---|---|---|---|
| Top view | Side view | Top view | Top view |
| Micro_Fin_n1 | | | |
| | | | |
| Micro_Fin_n2 | | | |
| | | | |
| Micro_Fin_n3 | | | |
| | | | |
| Micro_Fin_n4 | | | |

In the present study, the capillary wicking behavior was evaluated for HFE-7100 (3M™ Novec™) by using the same technique presented by Ahn et al. [10], Rahman et al. [11] and replicated by Cao et al. [3]. The capillary-wicking test consists of a modified surface slowly raised to contact a pendant fluid droplet attached to a small diameter capillary tube. As the surface contacts the liquid droplet, the fluid is wicked into the surface structure and the volumetric flow rate is measured by monitoring the liquid meniscus in the tube.

The experimental layout is shown in Fig. 2 where the capillary tube had 1 mm in diameter. The z-axis raised the surface until it touched the tube while the high-speed *Photron SA3* camera with a 100 mm MACRO lens recorded the meniscus displacement. After that, tracking image software was used to measure the liquid column variation inside the capillary tube and, then, the volume wicked was calculated. Table 2 shows the volume wicked by the surface at the first 50 milliseconds.

17
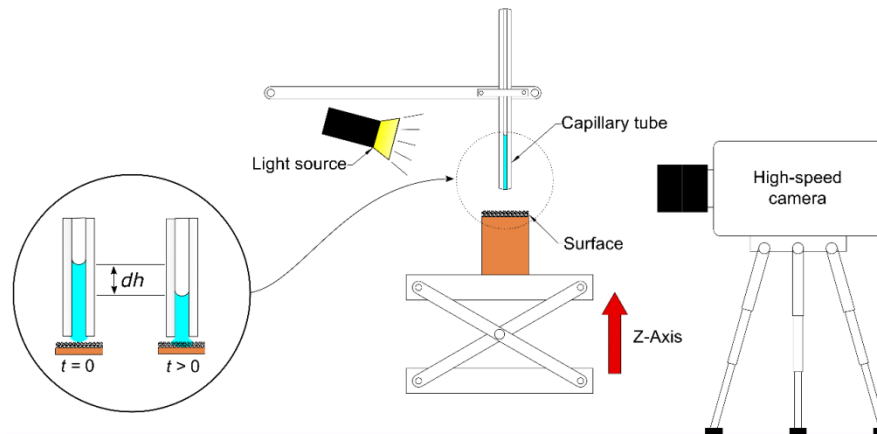
**Fig. 2** Schematic of the experimental device used for the wickability measurements.

One may observe that the microstructure surfaces have a greater capacity to absorb liquid than a flat surface. However, when evaluated among micro-fins surfaces it is not possible to notice any difference.

**Table 2** Micro-fins surfaces capillary wicking.

Micro_Fin_n3 (M3)

0 ms          10 ms          50 ms

Micro_Fin_n4 (M4)

0 ms          10 ms          50 ms
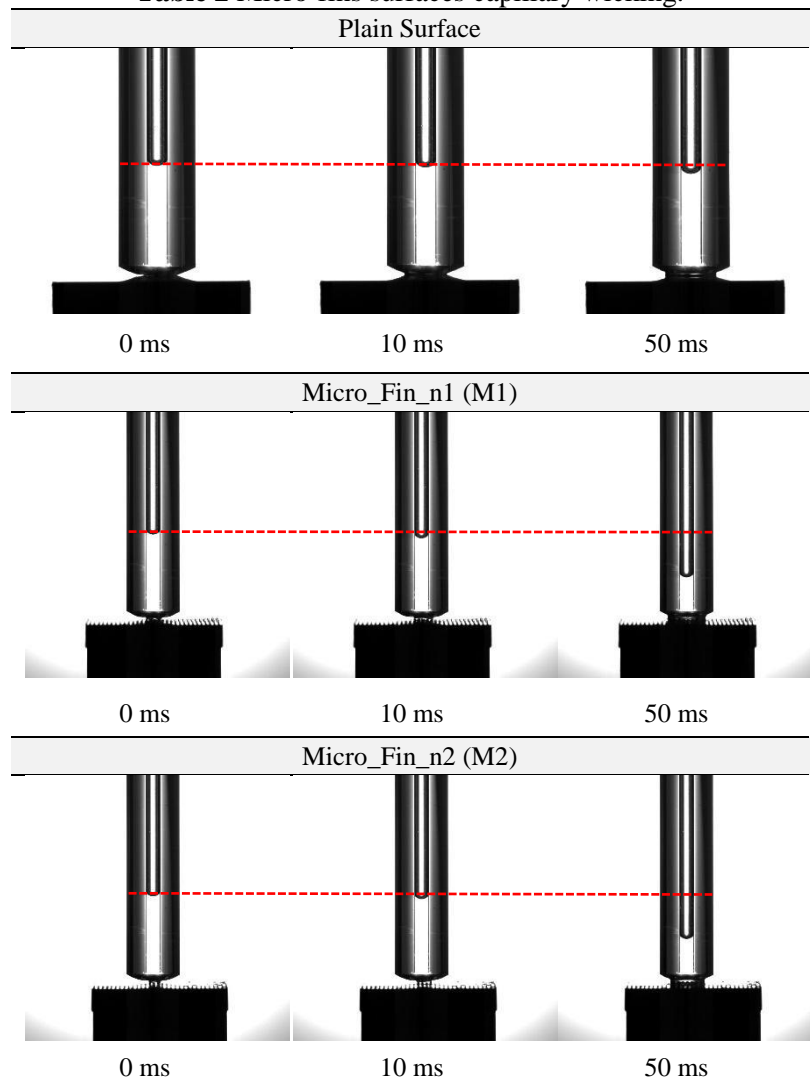
## 3. EXPERIMENTAL SETUP

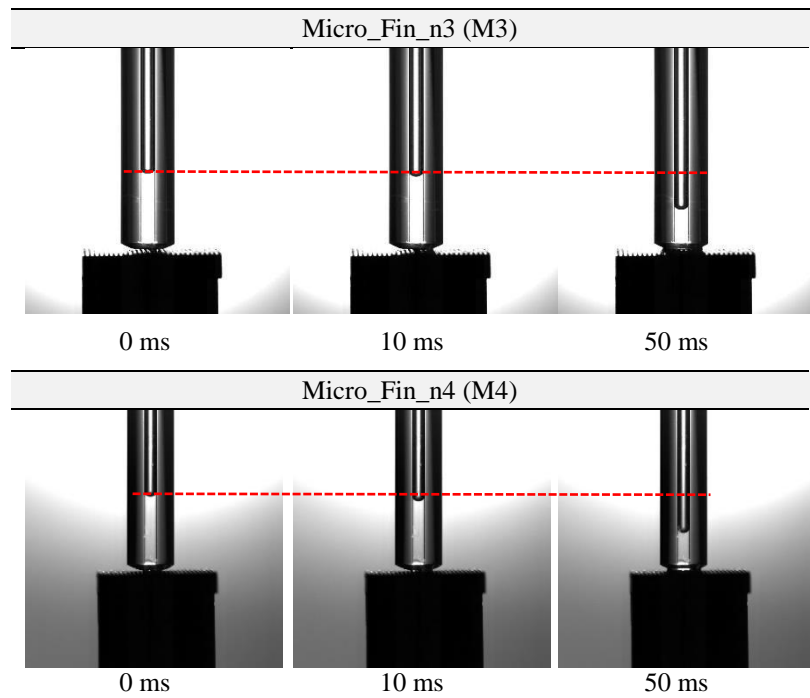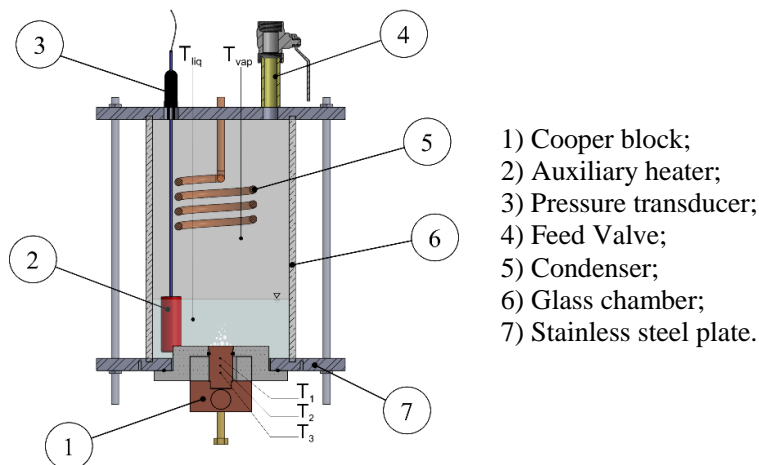The pool boiling apparatus used in the tests is shown in Fig. 3, which consisted of a rectangular chamber made of glass. In order to monitor the test fluid temperature, it was used two K-type thermocouples ($T_{liq,}$ and $T_{vap}$) located in the liquid and vapor regions, respectively. The pressure inside the boiling chamber was measured by an absolute pressure transducer Omega PXM309-2A (the experiments were performed under local atmospheric pressure, $p_{atm} = 98 \pm 0.05$ kPa).

The test section consisted of a copper piece with a square plate on the upper surface ($16 \times 16 \times 3$ mm) machined on a copper block with 60 mm height and 16 mm diameter (test section was machined from a unique copper piece in order to avoid thermal contact resistances). Three K-type thermocouples ($T_1$, $T_2$, and $T_3$) were embedded within the cylinder and this, in turn, was fixed on a second copper block containing a heater cartridge responsible for heating the test section. The test section was thermally insulated from the environment by a polytetrafluoroethylene (PTFE) piece.



1) Cooper block;
2) Auxiliary heater;
3) Pressure transducer;
4) Feed Valve;
5) Condenser;
6) Glass chamber;
7) Stainless steel plate.

**Fig. 3** Pool boiling apparatus.

A smooth plain surface ($R_a = 0.14$ µm), obtained by using the polishing method presented by Manetti et al. [12], was used as a reference surface.

An auxiliary heater was used to maintain the liquid temperature near the saturation conditions (a cartridge resistance with a maximum power of 350 W at 220 V submerged in the working fluid). Before each run, the auxiliary heater boiled the working fluid for 1 hour to eliminate noncondensing gases.

The boiling tests were performed by using HFE-7100 (3M™ Novec™) at saturation conditions. The test conditions were adjusted by monitoring the pressure and temperature inside the boiling chamber. For each test surface, at least two experiments were performed under similar conditions to ensure repeatability of results.

A data acquisition system (Agilent 34970A) was used to obtain all signals. The heat flux and surface temperature were calculated according to Fourier's Law, assuming 1-D conduction based on wall temperature measurements. The HTC was calculated using Newton's law of cooling, given by Eq. 1:

$$h = \frac{q''_{measured}}{T_w - T_{sat}(p_{int})} = \frac{q''_{measured}}{\Delta T_{sat}} \tag{1}$$

where $T_{sat}(p_{int})$ corresponds to the saturation temperature of the HFE-7100 evaluated at the pressure inside of the boiling chamber, and $T_w$ is the surface temperature, determined by extrapolating the linear temperature profile provided by the thermocouples allocated in the copper block. Different linear temperature curve fittings, with $R^2$ always higher than 0.99, were obtained for each heat flux based on the temperature measurements. Figure 4 shows the temperature profile and fitting curves obtained for each thermocouple.
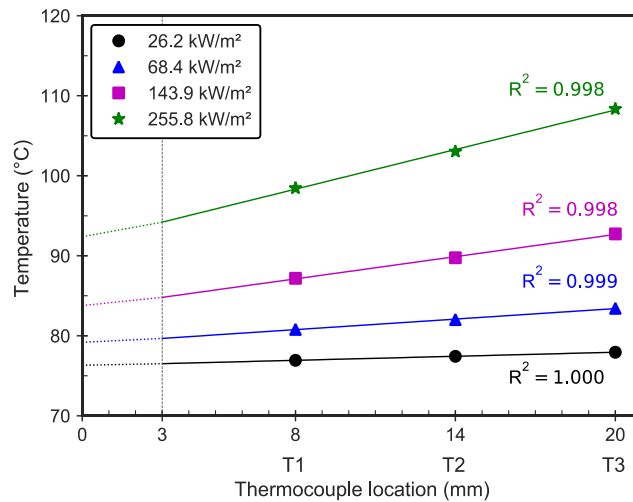


**Fig. 4** Example of linear temperature profiles used to estimate the heat flux and wall temperatures.

The linear temperature profile validates the assumption that heat losses in the radial direction are negligible. In addition, Fig. 5 presents the comparison between the imposed heat flux and the estimated heat flux from the linear profile, showing heat losses lower than 15% for all tests.
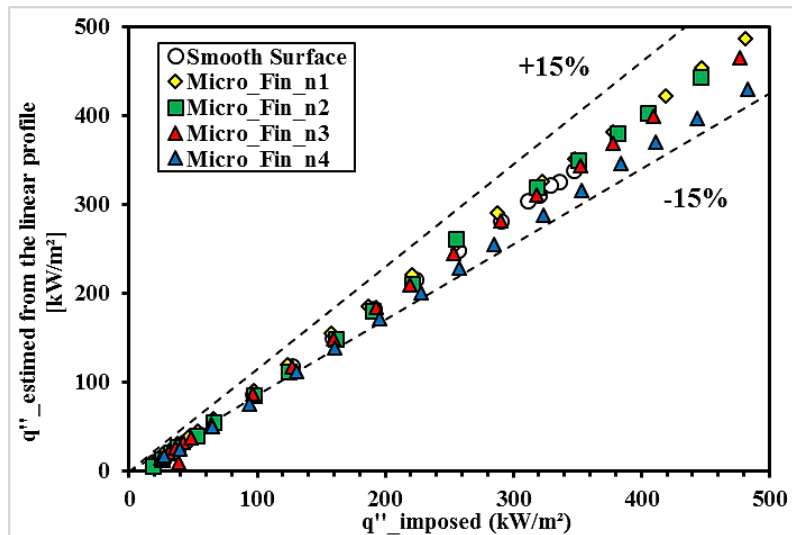
**Fig. 5** Heat flux estimated from the linear profile *versus* imposed heat flux.

The experimental uncertainties are estimated by using the method described by Moffat [13]. For all surfaces tested, the experimental uncertainty for the heat flux and the heat transfer coefficient varied from 10 to 2.6 % and from 10.7 to 4.7 %, respectively.

## 4. RESULTS AND DISCUSSION

The boiling heat transfer behavior for HFE-7100 at saturated conditions is presented in Fig. 6. One may observe that the micro-fin surfaces intensify the HTC and delay the dryout heat flux as compared to the plain surface.
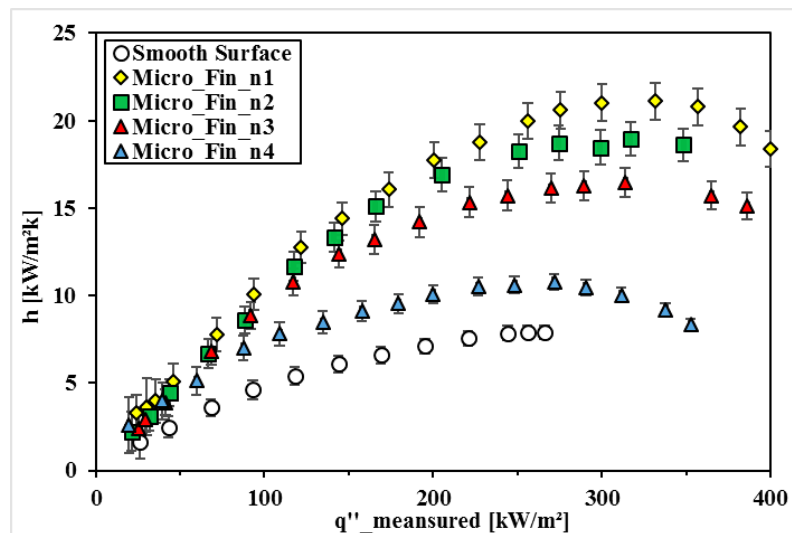


**Fig. 6** Heat transfer performance for micro-fins and plain surfaces and for HFE-7100 at saturated conditions.

Figure 7 summarizes the micro-fins parameters that can influence the pool boiling heat transfer. The presence of the micro-fins increases the surface heat exchange area, leading to an increase in the heat transfer coefficient as compared to the plain surface. From the parameters analyzed in this study, the number of fins seems to be responsible for the HTC enhancement. The surfaces 'Micro_Fin_n1' and 'Micro_Fin_n2' with 1024 fins have higher heat transfer coefficients than 'Micro_Fin_n3' and 'Micro_Fin_n4', with 841 micro-fins.
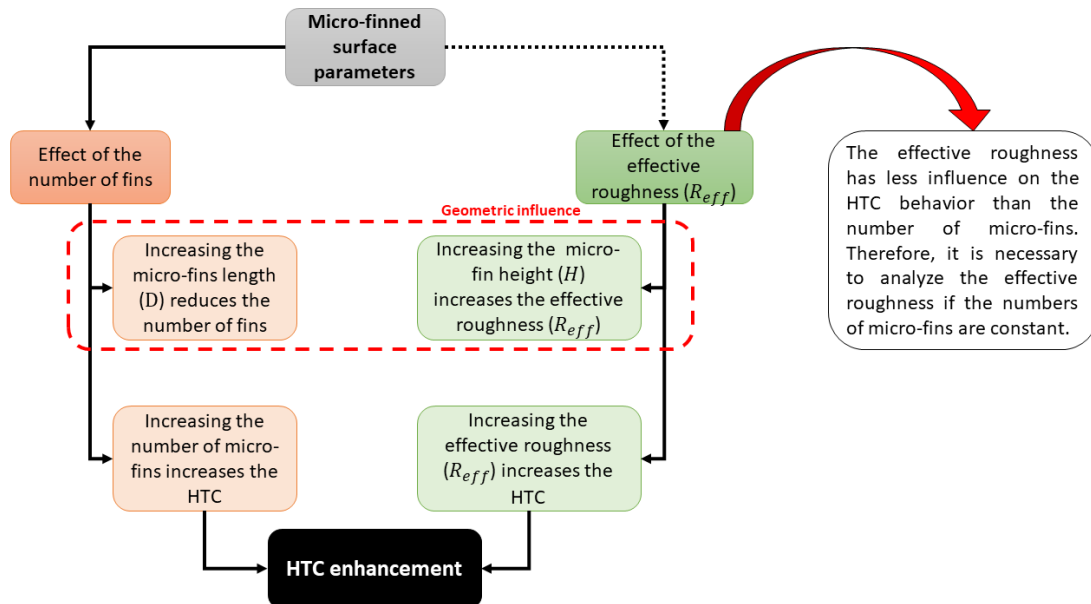
**Fig. 7** Micro-finned surface parameters that can influence on pool boiling heat transfer.

However, if the numbers of micro-fins are constant, it is necessary to analyze the effective roughness or roughness factor, defined by the relation between the surface area and the projected area; thus, the larger the effective roughness, the higher the heat transfer performance.

The roughness factor is not the main parameter responsible for the HTC deterioration/enhancement. This conclusion arises from the analysis of Fig. 1, which shows that the $R_{eff}$ value obtained by Chu et al. [9] is the same for the surfaces 'Micro_Fin_n1' and 'Micro_Fin_n3' and for the surfaces 'Micro_Fin_n2' and 'Micro_Fin_n4'; however, both sets of data present different values for the heat transfer coefficient. By analyzing the relation given by Chu et al. [9], it is evident that it is possible to obtain identical values for $R_{eff}$ only by adjusting the sample sizes. Thus, it is better to evaluate the influence of the fins length ($D$) and height ($H$) on the heat transfer.

In this study, the inter-fin space ($S$) was previously set; in this way, the length and the height of the micro-fins were varied. As the original dimensions of the copper surface were fixed ($16 \times 16$ mm), an increase in the micro-fins length results in a reduction in the number of fins, leading to HTC degradation. When we compare two surfaces with the same fin length, which means that both have the same number of micro-fins, the tallest fin will present the highest HTC. This is due to the lateral edges of the fins allowing a larger contact area with the liquid.

## 5. CONCLUSION

This study evaluated experimentally the thermal performance of different micro-fin surfaces by using HFE-7100, at saturated condition, as working fluid. Micro-fin surfaces intensify the HTC as compared to the plain surface and the number of fins seems to be the main factor for this enhancement (for $q'' = 250$ kW/m², 'Micro_Fin_n1' showed an increase of 260% in the HTC as compared to the plain surface); the presence of gases trapped at the fin base reduces the energy required for the onset nucleate boiling, increasing the number of nucleation sites and, consequently, the heat transfer performance.

Another parameter analyzed is the effective roughness, which has less influence on the HTC behavior than the number of fins. If the number of micro-fins is constant, the larger the effective roughness the higher the heat transfer performance.

Additionally, the capillary-wicking ability increases for micro-fin surfaces, improving the HTC and delaying the dryout heat flux due to the prevention of hotspots on the heating surface. Thus, the surface thermal behavior is a function of the surface morphology and its surface capillary wicking.

## ACKNOWLEDGMENT

## NOMENCLATURE

| | | | | | | |
|---|---|---|---|---|---|---|
| CHF | Critical heat flux | (kW/m²) | $S$ | Inter-fin space | (µm) |
| $D$ | Side length of pillars | (µm) | $T_1, T_2, T_3$ | Temperature copper block | (°C) |
| $H$ | Height of pillars | (µm) | $T_{liq}$ | Liquid temperature | (°C) |
| $h$ | Heat transfer coefficient | (W/m²K) | $T_{vap}$ | Vapor temperature | (°C) |
| $q''$ | Heat flux | (kW/m²) | $T_{sat}$ | Saturation temperature | (°C) |
| $R_a$ | Average roughness | (µm) | $T_w$ | Wall temperature | (°C) |
| $R_{eff}$ | Effective roughness | ( - ) | | | |

## REFERENCES

[1] Demir, E., Izci, T., Alagoz, A.S., Karabacak, T., Kosar, A. "Effect of silicon nanorod length on horizontal nanostructured plates in pool boiling heat transfer with water". *International Journal of Thermal Sciences*, v. 82, pp. 111-121, (2014).

[2] Liang, G.; Mudawar, I. "Review of pool boiling enhancement by surface modification". *International Journal of Heat and Mass Transfer*, v. 128, p. 892-933, (2019).

[3] Cao, Z., Liu, B., Preger, C., Wu, Z., Zhang, Y., Wang, X.; Sundén, B. "Pool boiling heat transfer of FC-72 on pin-fin silicon surfaces with nanoparticle deposition". *International Journal of Heat and Mass Transfer*, v. 126, p. 1019-1033, (2018).

[4] Dong. L., Quan, X., Cheng, P. "An experimental investigation of enhanced pool boiling heat transfer from surfaces with micro/nano-structures". *International Journal of Heat and Mass Transfer*, v.71, pp. 189-196, (2014).

[5] Sinha-Ray, S., Zhang, W., Sahu, R. P., Sinha-Ray, S., Yarin, A. L. "Pool boiling of Novec 7300 and DI water on nano-textured heater covered with supersonically-blown or electrospun polymer nanofibers", *International Journal of Heat and Mass Transfer*, v.106, p. 482-490, (2017).

[6] Cooke, D., Kandlikar, S.G. "Effect of open microchannel geometry on pool boiling enhancement", Int. J. Heat Mass Transfer, v. 55, pp. 1004-1013, 2012.

[7] Kim, B, S., Lee, H., Shin, S., Choi, G., Cho, H, H. "Interfacial wicking dynamics and its impact on critical heat flux of boiling heat transfer", Appl. Phys. Lett., v.105, p.19160, 2014.

[8] Kim, S.H., Lee, G.C., Kang, J.Y., Moriyama, K., Kim, M.H., Park, H.S. "Boiling heat transfer and critical heat flux evaluation of the pool boiling on microstructured surface", Int. J. Heat Mass Transfer, v.91, pp. 1140-1147, 2015.

[9] Chu, K-H., Enright, R., and Wang, E. N. "Structured surfaces for enhanced pool boiling heat transfer". *Applied Physics Letters*, v. 100, n. 24, p. 241603, (2012).

[10] Ahn, H.S., Park.G., Kim, J.M., Kim.J., Kim, M.H. "The effect of water absorption on critical heat flux enhancement during pool boiling", Exp. Therm. Fluid Sci., v. 42, pp.187-195, 2012.

[11] Rahman, M.M., Olçeroglu, E., McCarthy.M. "Role of wickability on the critical heat flux of structured superhydrophilic surfaces", Langmuir, v.30, pp. 11225-11234, 2014.

[12] Manetti, L.L., Mogaji, T.S., Beck, P.A., Cardoso, E.M. "Evaluation of the heat transfer enhancement during pool boiling using low concentrations of $Al_2O_3$ -water based nanofluid", *Exp. Therm. Fluid Sci*. v.87, p. 191 – 200, (2017).

[13] R.J. Moffat, "Describing the Uncertainties in Experimental Results", p. 3–17. (1988).